Chapter 7
Reevaluating the Role of Water in Plasma-assisted Nitrogen Fixation

Mikhail Gromov, Mehrnoush Narimisa, Rino Morent, Rony Snyders, and Nathalie De Geyter

Abstract Global population growth accelerated significantly in the early twentieth century, increasing from approximately 1.6 billion in 1900 to over 2.5 billion by 1950. This growth coincided with the discovery of artificial nitrogen fixation methods. The Haber-Bosch process, the primary method for ammonia synthesis (NH_3) and nitrogen-containing fertilizers relies on natural gas (CH_4), bringing significant environmental and economic challenges. A shift toward sustainable, low-CO_2 fertilizer production is necessary, with non-equilibrium plasma technology offering a promising green alternative for local nitrogen fixation. However, the use of water as a hydrogen source in plasma-based nitrogen fixation presents specific challenges related to physics (electron energy distribution and interaction) and chemistry (reaction pathways), which directly impact process efficiency and product yield. This chapter discusses the underlying scientific problems and explores the challenges and the role of water in plasma-based nitrogen fixation from the perspectives of physics, chemistry, and engineering.

M. Gromov (✉)
Research Unit Plasma Technology (RUPT), Department of Applied Physics, Ghent University, Ghent, Belgium

Leibnitz Institute of Plasma Science and Technology, Greifswald, Germany
e-mail: Mikhail.Gromov@inp-greifswald.de; Mikhail.Gromov@UGent.be

M. Narimisa · R. Morent · N. De Geyter
Research Unit Plasma Technology (RUPT), Department of Applied Physics, Ghent University, Ghent, Belgium
e-mail: Mehrnoush.Narimisa@UGent.be; Rino.Morent@UGent.be; Nathalie.DeGeyter@UGent.be

R. Snyders
Chimie des Interactions Plasma-Surface (ChIPS), CIRMAP, Mons University, Mons, Belgium

Materia Nova Research Centre, Parc Initialis, Mons, Belgium
e-mail: Rony.SNYDERS@umons.ac.be

S. K. Guharay, M. Wada (eds.), *Emerging Applications of Ions and Plasmas*,
Springer Series on Atomic, Optical, and Plasma Physics 127,
https://doi.org/10.1007/978-3-031-84245-0_7

7.1 Introduction

Nitrogen is essential for forming proteins, nucleic acids, and other cellular constituents that are crucial for life. Although abundant in air as N_2, its stable triple bond makes it inert. Nitrogen fixation (NF) converts N_2 into reactive forms like ammonium (NH_4^+) or nitrate (NO_3^-) ions, which organisms can use. However, natural NF processes, such as those performed by soil bacteria and lightning, cannot meet the growing food production demands of the increasing human population.

During harvest, nitrogen is removed from the soil along with crops, a process called soil denitrification, leading to crop growth issues. Adding nitrogen-containing fertilizers (N-fertilizers) replenishes soil nitrogen and boosts yields, but overuse can emit greenhouse gases like N_2O, which is toxic and harmful to human health. Thus, managing nitrogen levels is critical for sustainable agriculture and environmental health [1–4]. In this regard, it has been recognized as one of the 14 grand challenges for engineering in the twenty-first century, which requires decisive actions [5].

The Haber-Bosch (HB) process for ammonia (NH_3) production is one of the main industrialized chemical processes that have been frequently prescribed as the main reason for the rapidly growing human population during the last century [6, 7]. NH_3 is synthesized from N_2 and H_2 gases (7.1) in the presence of an iron-based catalyst, as shown in Fig. 7.1a. Pure N_2 is typically obtained utilizing cryogenic distillation of air. Natural gas (CH_4) is normally used as an H feedstock as well as to provide energy for creating the high pressure (200 atm) and temperature (> 700 K) required for the synthesis. In a next step, the gas is cooled down, compressed, and condensed, obtaining fluid NH_3 as the output.

$$N_2 + 3H_2 \rightarrow 2NH_3 \tag{7.1}$$

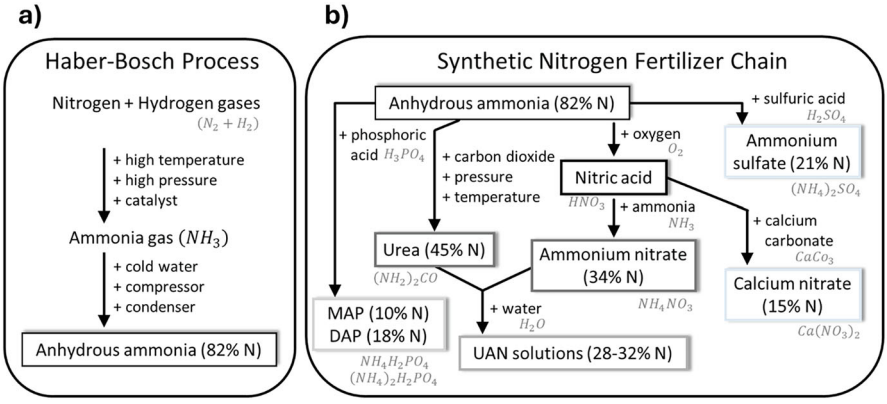

Fig. 7.1 Diagram of the Haber-Bosch process (**a**) and a simplified scheme showing different N-fertilizers and products obtained from anhydrous ammonia (**b**)

An abundant content of N in anhydrous ammonia (~82%) makes it suitable for being the basic component of N-fertilizer production, reducing storage and distribution costs. Figure 7.1b shows different N-fertilizers produced from NH_3. Urea and ammonium nitrate lead the agricultural market owing to their relatively simple production and high N content. The latter is synthesized using ammonia and nitric acid (HNO_3), which in turn is also produced from NH_3 via the Ostwald process according to the following reaction [8]:

$$2NH_3 + 4O_2 + H_2O \rightarrow 3H_2O + 2HNO_3 \tag{7.2}$$

The numerous usage of NH_3 makes the HB process the largest global energy (~2%) and natural gas consumer (~3–5%), leading to enormous greenhouse gas emissions (> 400 million metric tons per year of CO_2, which is according to statistics from 2021 more than 1/3 of the yearly CO_2 emissions from the chemical industry combined [9, 10]). Moreover, the process is only profitable on a large industrial scale that requires a well-developed distribution network. In addition, anhydrous ammonia is stored and distributed as a liquid that requires special high-pressure equipment (barrels), creating additional storage and transportation expenses. Nowadays, the HB process energy consumption is 0.48 MJ/mol of NH_3, which is very close to its theoretical minimum of 0.38 MJ/mol of NH_3 [11]. The current upgrade strategy is mainly related to decreasing natural gas consumption, for instance, replacing it with water as a green source of H or using another catalyst that can reduce reaction temperature and pressure. However, at the same time, the use of water increases the energy cost by a factor of 3 (1.5 MJ/mol), while a new catalyst has not been found yet [12, 13].

With such a multilateral problem, it is not straightforward to identify the effort that will make the biggest impact. It has been considered that when a fertilizer could meet the demand close to the field only when the crop needs it, nutrient loss and N-pollution would be reduced. An example of this is a split application that reduced the N emissions by 25% [14]. Thus, we can conclude that the core of the N-cycle problem is the current paradigm of how we produce and apply N-containing fertilizers. One of the possible solutions is to ensure a sustainable and eco-friendly small-scale process, which is compatible with renewable energy sources and independent of any rare resources, producing fertilizers directly in the place where they will be used.

To address the environmental and other concerns associated with the N-fertilizers industry, researchers aim to develop an alternative method of NF, where even a minor improvement toward more efficient synthesis multiplied by world scale can bring significant benefits. Various NF methods show promising results. These include reconsidering the HB process or developing alternative, complementary processes for NF, such as enzyme-based, plasma-based, and (electro-)catalytic methods with both heterogeneous and homogeneous catalysts [12, 15, 16]. Among the different techniques mentioned, plasma-based NF is particularly appealing because of its flexibility and synergy with sustainable energy sources [17]. Moreover, theoretical estimations demonstrate that certain plasmas can ensure 2.5 times more

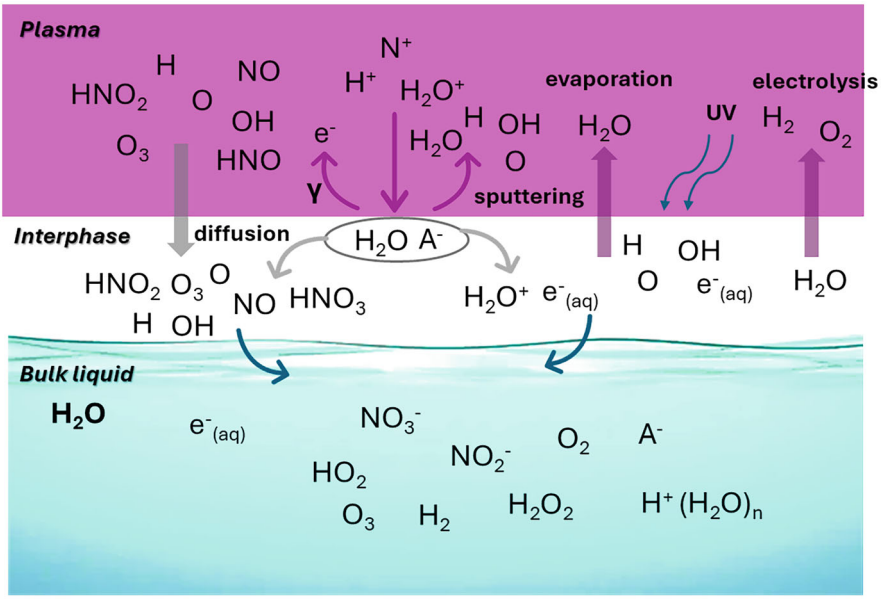

Fig. 7.2 Schematic overview of some important processes at the plasma–liquid interface. More details can also be found in [58]

energy-efficient NF than the currently used HB process [18], as will be discussed in the next section.

Both NH_3 and HNO_3 production require a source of H, which current industrial processes obtain by the steam reforming of methane (CH_4), resulting in substantial CO_2 emission. A direct plasma-based conversion of $N_2 + CH_4$ appears to be an appealing alternative for NH_3 synthesis [19]. Bioethanol (bio-EtOH) is another interesting candidate as a hydrogen carrier in the form of C-H and O-H radicals [20, 21]. However, neither CH_4 nor EtOH aligns with the initial concept of green NF because they contain carbon, and their use contradicts the decarbonization goals pursued by many countries. Nevertheless, the NH_3 formation chemistry in $N_2 + CH_4$ or EtOH mixtures is of scientific interest because value-added side products can also be formed (H_2, C_xH_y), challenging the selectivity toward NF [22].

Considering the pivotal impact of CH_4 as an H source, it is suggested to use water as a more eco-friendly solution despite losing the HB process's energy efficiency [11]. At the same time, plasma-based NF can offer an alternative route for NH_3 and HNO_3 manufacture, using only air and water as feedstock. However, while the presence of water is essential for product formation and accumulation, its effect on nitrogen fixation performance, including energy cost, production rate, and selectivity, remains unclear and is the subject of ongoing debates.

Figure 7.2 schematically shows the plasma–liquid interaction process, including the main reactive species and products. In the context of NF in the presence of H_2O, there is no consensus on the reaction locus. Researchers are divided, with some

attributing the reactions to the gas phase, others to the plasma–liquid interface, and still others to the liquid phase. It is well established that enhancing the plasma–liquid surface area can significantly boost the production rate of NF species [20]. This has led to extensive studies on designs that increase interface surface area, such as aerosol droplets [23], water films, vapor [24], and plasmas with larger plasma–liquid interaction surface [20].

The exact source of the reactive species driving plasma–liquid chemistry remains a topic of debate. For plasma jets interacting with liquid water, conflicting results from various research groups suggest that plasma may or may not directly interact with liquid water molecules. The formation of NH_x and NO_x species by N_2-containing plasma over water has been proposed to occur either in the gas phase from evaporated water [23, 24] or through direct interaction of plasma species with the top layer molecules of liquid H_2O [25, 26]. Therefore, the nature of plasma interaction with liquid likely depends on the specific plasma–liquid system, including the gaseous discharge properties and the geometry of the plasma–liquid interface.

From plasma physics standpoint, the effect of water on plasma generation, plasma sustaining, and energy distribution among the reactants is also very important and often overlooked, as will be discussed in the following sections. This includes the interaction of water with excited species that drive the chemistry, the water activation processes, and the transfer of H_2O from the liquid to the gas phase (evaporation).

Considering that the water presence in the plasma can change the physics and chemistry of plasmas, it is rather difficult to theoretically estimate what system with or without water's presence is more effective for NF. Unfortunately, most of the works reported in the literature are dedicated to either "dry" plasmas [27–30] or plasmas with water present in the form of the liquid electrode [31, 32], vapor [33, 34], or underwater discharges [35], rendering their direct comparison difficult, if not impossible. Therefore, due to the versatility of the water effect on plasma-based nitrogen fixation, this chapter aims to provide comprehensive knowledge in an easily accessible format, discussing fundamentals and chemical pathways of plasma-based NF in the presence of water.

7.2 Fundamentals of Plasma-Based Nitrogen Fixation

7.2.1 Equilibrium Plasmas vs. Non-Equilibrium Plasma and Their Difference

Plasmas can be divided into local thermodynamic (or thermal) equilibrium plasmas (LTE) and non-local thermodynamic equilibrium plasmas (non-LTE) [36]. LTE or thermal plasmas are governed by collisions, and every collision has to be balanced by its inverse process, i.e., excitation/deexcitation, ionization/recombination. In

this case, local gradients of plasma properties (temperature, density, and thermal conductivity) are sufficiently low to let particles in the plasma equilibrate. This means that in LTE plasmas, the temperature of heavy particles is close to the temperature of the electrons ($T_{electrons} = T_{heavy}$ ($T_{ions} = T_{gas}$)). In turn, deexcitation processes in non-LTE or non-thermal plasmas are characterized by significant radiative deexcitation, but not collisions. A considerable mass difference between electrons and neutral particles determines their acceleration in the applied electrical field. Light electrons preferentially take the energy from the field and collide with "heavy" neutrals (atoms/molecules), creating a manifold of highly energetic species, including atoms, ions, and excited states. Thus, non-LTE plasmas can be described by different energy distributions between energetic electrons and heavy particles as $T_{(electrons(e))} > T_{(ions(i))} > T_{(vibrational(v))} > T_{(rotational(r))} \geq T_{(translational(t))} = T_{(gas(g))}$. It is worth noting that T_v and T_r are characteristics of molecular plasmas because only molecules have vibrational and rotational degrees of freedom.

The main elementary processes initiated in plasma, which make it attractive for gas conversion chemistry, are schematically presented in Table 7.1. Electrons are the first to receive energy from the electric field in a plasma due to their small mass (e.g., $m_{hydrogen}/m_{electron} = 1840$), and they distribute it among the other plasma components. The main electron-initiated processes are P1–P7 as given in Table 7.1. These processes are generally divided into two groups, representing elastic and inelastic collisions. The first group, described as P1, changes the kinetic energy of the neutral species and is attributed to gas heating (dominant in thermal plasmas). The second group, P2–7, creates a manifold of highly reactive species that can initiate unique plasma chemistry (dominant in non-thermal plasmas). These inelastic collisions between electrons and "heavy" particles can dissociate

Table 7.1 Elementary processes in plasmas

Process		Scheme
P1	Momentum transfer	$\mathbf{AB + e^-(p_1) \rightarrow AB + e^-(p_2)}$
P2	Electron dissociation	$\mathbf{AB + e^- \rightarrow A + B + e^-}$
P2.1	"Heavy" particle dissociation	$\mathbf{AB^* + AB \rightarrow AB + A + B}$
P3	Excitation	$\mathbf{AB + e^- \rightarrow AB^* + e^-}$
P3.1	Electronic excitation	$\mathbf{AB(g, E_i) + e^- \rightarrow AB(E_j) + e^-}$
P3.2	Vibrational excitation	$\mathbf{AB(g, v_i) + e^- \rightarrow AB(v_j) + e^-}$
P3.3	Vibrational-vibrational energy exchange	$\mathbf{AB(v_i) + AB(v_j) \rightarrow AB(v_i - n) + AB(v_j + m)}$
P3.4	Vibrational-translational energy exchange	$\mathbf{AB(v_i) + M \rightarrow AB(v_i - n) + M}$
P4	Electron ionization	$\mathbf{AB + e^- \rightarrow AB^+ + 2e^-}$
P4.1	"Heavy" particle ionization	$\mathbf{AB + C^+ \rightarrow AB^+ + C}$
P5	Dissociative attachment	$\mathbf{AB + e^- \rightarrow A^- + B}$
P6	Detachment	$\mathbf{A^- + e^- \rightarrow A + 2e^-}$
P7	Dissociative ionization	$\mathbf{AB + e^- \rightarrow A^+ + B + 2e^-}$
P8	Photon emission	$\mathbf{AB(E_j) \rightarrow AB(E_i) + \mathit{hv}}$

molecules (P2), modify the electronic structure of the neutral species, i.e., excite (P3, electronically (E) and/or vibrationally (v)) or ionize (P4) them, and can lead to electron attachment/detachment (P5–P7).

Electron collisions with "heavy" particles, which lead to the formation of excited species, have a particular interest in gas conversion (P3.1–P3.4). This is because these formed species can also have enough energy to overcome a reaction's activation energy barrier (E_a) and take the role of electrons, initiating similar processes. For example, electrons can transfer their energy to another species, resulting in the formation of ions (P4, e.g., N_2^+), electronically excited (P3.1, e.g., $N_2(A, B, C)$, and vibrationally excited species (P3.2, e.g., $N_2(X, v)$), depending on the electron energy in the moment of the collision. These energetic "heavy" particles will also transfer their energy in processes such as P2.1 and P4.1, significantly contributing to gas transformation. However, the same energetic species can also exchange (more often lose) their energy in vibrational–vibrational (V-V, P3.3) and vibrational–translational (V-T, P3.4) energy exchange reactions, through which vibrational energy is transferred to heat or lost by radiation (P8, spontaneous emission process). Processes P6 and P7 are mostly considered in low-pressure plasmas.

It is reasonable to ask: "What are the chances that electrons or excited "heavy" particles will react with one or another component of the gas mixture?". The amount of energy going into each possible energy transfer process between electrons and atoms/molecules, i.e., electronic excitation, vibrational excitation, dissociation, and ionization, is determined by a reaction threshold energy (in [eV]), and cross-section (in [m^2]). The threshold energy depends on a "heavy" particle that an electron collides with and determines the minimum energy that the electron has to have to activate one of the processes. The cross-section defines the probability of the process and varies with electron energy. Finally, the electron energy is determined by the reduced electric field strength, which is the ratio of the electric field E over gas number density n (E/n), and described by the electron energy distribution function (EEDF), i.e., the portion of the electrons with a specific energy, or T_e. Consequently, one can often control the plasma chemistry by influencing the electron parameters, namely, density, temperature, and EEDF.

7.2.2 Plasma-Based Nitrogen Fixation and the Governing Species

The most energy-demanding and rate-limiting step of NF is the activation process of an inert N_2 molecule whose first dissociation limit is at 9.76 eV, as shown in Fig. 7.3a. Plasmas can offer several mechanisms, leading to N_2 activation, i.e., its dissociation or creating N_2 with abundant energy that can further react with other gas mixture components.

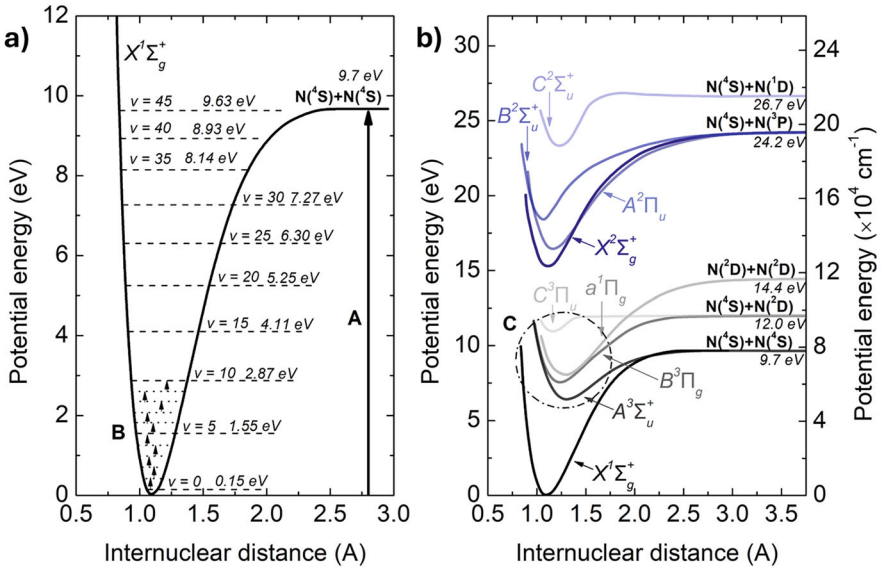

Fig. 7.3 (**a**) N_2 ground state energy diagram showing the vibrational structure; (**b**) potential energy curves of N_2 and N_2^+ electronic states. The energy diagrams were built based on the constants provided in [38]

7.2.2.1 Thermal Activation

Thermal energy is directly tied to the kinetic energy of gas molecules. As temperature increases, the average kinetic energy of N_2 molecules rises, enabling more collisions to break the strong triple bond. Thus, thermal N_2 dissociation is a high-energy process.

7.2.2.2 Direct Electron Impact Dissociation

The first N_2 dissociation limit is at 9.76 eV, as shown in Fig. 7.3a. The reaction (7.3) can potentially take place if the electron has an energy of more than 9.76 eV (process marked as "A" in Fig. 7.3a). In this way, the direct electron dissociation will compete with the electronic excitation of N_2 (7.3 vs. 7.4), and because their energy levels are very close, as shown in Fig. 7.3b (the region marked as "C"), the dissociation will be minor. Thus, the electron excitation process cross-section is several orders of magnitude higher than direct electron impact [37].

$$e + N_2 \rightarrow N + N + e \tag{7.3}$$

$$e + N_2 \rightarrow N_2^*(E) + e \tag{7.4}$$

where * denotes excitation and "E" stands for electronic excitation, which in the case of N_2 can, most probably, be $A^3\Sigma_u^+$, $B^3\Pi_g$, $a^1\Pi_g$, or $C^3\Pi_u$ electronically excited states.

7.2.2.3 N_2 Activation via Vibrational Ladder Climbing

This mechanism is initiated by low-energy electrons that can vibrationally excite N_2 (7.5), as shown in Fig. 7.3a, marked "B." These $N_2(X^1\Sigma_g^+, v)$ states can also exchange energy with each other (7.6), forming $N_2(X^1\Sigma_g^+, v')$ with a high vibrational number. This process is called vibrational ladder climbing. The energy of $N_2(X^1\Sigma_g^+, \Delta v = 1)$ is <0.3 eV and decreases with every next level according to the anharmonic oscillator theory (more information about the N_2 electronic structure is presented further on in Table 7.2) [39]. These states can exist for a long time due to their low vibrational relaxation constant ($k = 10^{-24}$–10^{-25} m^3s^{-1}) [18, 40] and can lower the N_2 dissociation limit in direct electron impact reactions according to 7.7. Unfortunately, in real plasmas, the vibrational energy relaxation in vibrational-translational (V-T) energy exchange processes (P3.4, Table 7.1) is significant, leading to gas heating, and strongly depends on the pressure. This challenges the vibrational ladder climbing mechanism, decreasing the population of $N_2(X^1\Sigma_g^+, v > 0)$. Moreover, V-T relaxation accelerates with temperature and vibrational state numbers. This is why the most pronounced vibrational excitation is observed in low-pressure plasmas, where V-T processes are slower due to fewer collisions. At high pressure, the formation of high vibrational levels is accompanied by gas heating and suppressed, making it difficult to distinguish its role in NF from thermal mechanisms [18, 41–43].

$$e + N_2\left(X^1\Sigma_g^+, v = 0\right) \rightarrow N_2^*\left(X^1\Sigma_g^+, v > 0\right) + e \tag{7.5}$$

$$\begin{aligned} N_2^*\left(X^1\Sigma_g^+, v \neq 0\right) + N_2^*\left(X^1\Sigma_g^+, v \neq 0\right) \rightarrow N_2^*\left(X^1\Sigma_g^+, v + n\right) \\ + N_2^*\left(X^1\Sigma_g^+, v - n\right) \end{aligned} \tag{7.6}$$

$$e\,(E_e < 9,76eV) + N_2\left(X^1\Sigma_g^+, v \neq 0\right) \rightarrow N + N^{(*)} + e, \tag{7.7}$$

7.2.2.4 N_2 Activation Through Electronic Excitation

Electrons with energy from 6.17 to 12 eV can electronically excite N_2, as shown in Fig. 7.3b and Table 7.2. These N_2 electronically excited states may further interact with other gas mixture components and lead to N_2 dissociation as well as dissociation of other gas components (process P2.1 in Table 7.1). At the same time,

Table 7.2 Typical activated species in air and humid air plasmas [37, 44–46]

N_2		N		N_2^+	
Electronic state	Potential energy, eV	Electronic state	Potential energy, eV	Electronic state	Potential energy, eV
$N_2\left(X^1\Sigma_g^+\right)$	0	$N(^4S)$	0	$N_2^+\left(X^2\Sigma_g^+, v\right)$	>15.45
$N_2\left(X^1\Sigma_g^+, \Delta v = 1\right)$	<0.3	$N(^2D)$	2.39	$N_2^+\left(A^2\Pi_u, v\right)$	>16.5
$N_2\left(A^3\Sigma_u^+, v\right)$	>6.17	$N(^2P)$	3.57	$N_2^+\left(B^2\Sigma_u^+, v\right)$	>18.35
$N_2(B^3\Pi_g, v)$	>7.35			$N_2^+\left(C^2\Sigma_u^+, v\right)$	>23.2
$N_2(a^1\Pi_g, v)$	>8.04				
$N_2(C^3\Pi_u, v)$	>11.03				
O_2		O		O_2^+	
$O_2\left(X^3\Sigma_g^-\right)$	0	$O(^3P_2)$	0	$O_2^+\left(X^2\Pi_g, v\right)$	>12.07
$O_2\left(X^3\Sigma_g^-, \Delta v = 1\right)$	<0.2	$O(^3P_1)$	>0.02	$O_2^+\left(a^4\Pi_u, v\right)$	>16.10
$O_2(a^1\Delta_g, v)$	>0.97	$O(^3P_0)$	>0.028	$O_2^+\left(A^2\Pi_u, v\right)$	>17.04
$O_2\left(b^1\Sigma_g^+, v\right)$	>1.63	$O(^1D_2)$	>1.97	$O_2^+\left(b^4\Sigma_g^-, v\right)$	>18.17
$O_2\left(c^1\Sigma_u^-, v\right)$	>4.08	$O(^1S_0)$	>4.19		
$O_2(A^1\Delta_u, v)$	>4.33				
$O_2\left(A^3\Sigma_u^+, v\right)$	>4.37				
H_2O		OH		H	
$H_2O(X^1A_1)$	0	$OH(X^2\Pi)$	0		
$H_2O\begin{pmatrix} X^1A_1, \\ \Delta v_1, \\ \Delta v_2, \\ \Delta v_3 \end{pmatrix}$	<0.45, <0.47, <0.2	$OH(X^2\Pi, \Delta v = 1)$	<0.44		
$H_2O(A(^1B_1), v)$	>6.67	$OH(A^2\Sigma^+, v)$	>4.04		
$H_2O(B(^1A_1), v)$	>8.79	$OH(B^2\Sigma^+, v)$	>8.61		
$H_2O(C(^1B_1), v)$	>10	$OH(C^2\Sigma^+, v)$	>11.1		
$H_2O(D(^1A_1), v)$	>10.17				

most of the N_2(E) states have a short lifetime (a few ns at atmospheric pressure for $N_2(B^3\Pi_g$ and $C^3\Pi_u)$ states and can lose their energy by radiation (P8 in Table 7.1, spontaneous emission process); thus, they have a limited contribution to NF. Meanwhile, metastable $N_2(A^3\Sigma_u^+$ and $a^1\Pi_g)$ states are relatively long-lived ones and can govern NF chemistry.

7.2.2.5 Energy-Favorable NF Mechanism

Table 7.3 presents the importance of N_2 activation mechanisms as a function of mean electron energy/reduced electric field (E/n) in a pure N_2 gas system [41]. It is worth noting that among the aforementioned mechanisms for N_2 activation, N_2^+

Table 7.3 The dominant electron energy loss mechanisms in N_2 atmosphere and typical plasma setups associated with various ranges of reduced electric field and mean electron energy

Reduced electric field (E/n) [Td] or mean electron energy [eV]	Dominant electron energy loss fraction	Typical representatives
<5 td or <0.2 eV	Momentum transfer (gas heating)	Thermal arcs, MW
5–100 td or 0.2–2 eV	Vibrational excitation	Glow discharges, MW, RF, gliding arc
100–1000 td or 2–10 eV	Electronic excitation	Corona, DBD, spark
>1000 td or >10 eV	Ionization and dissociation	Electron beam sources, high-energy laser-induced plasma

ions also possess sufficient energy to initiate N_2 activation, leading to its dissociation or reaction. However, N_2 activation through ionization can be neglected under high-pressure conditions due to the ions' extremely short lifetime.

For several reasons, NF driven by the vibrational ladder climbing mechanism is superior to direct electron dissociation or thermal dissociation because:

- It requires low E/n strength, corresponding to a mean electron energy of about 2 eV (see Table 7.3), resulting in reasonable energy consumption;
- Vibrational excitation decreases the N_2 dissociation energy in electron impact reactions following 7.7.
- Finally, an important reaction for N_2 oxidation: $N_2 + O \rightarrow NO + N$, having an E_a of 3.06 eV, can be initiated by vibrationally excited $N_2(X^1\Sigma_g^+, v > 12)$. As such, the mechanism can be more energy efficient compared to direct dissociation [18, 47–51].

Theoretical estimations based on the activation mechanism of N_2 by vibrational ladder climbing demonstrate that NF, namely oxidation, carried out via non-thermal plasmas can potentially be 2.5 times more efficient than the currently used HB process (0.2 and 0.48 MJ/(mol N), respectively) [12, 18]. In thermal chemical processes such as HB, achieving the necessary activation energy for reactions typically requires high temperatures and pressures. However, reverse processes may occur under such harsh conditions, thermodynamically limiting the overall process efficiency. In contrast, the aforementioned mechanism implemented in non-equilibrium plasmas can provide a way to overcome the thermodynamic limit of thermal chemical processes, and so is able to provide an alternative to the HB process and other catalytic pathways. Although the vibrational ladder climbing competes with vibrational energy relaxation in V-T processes, leading to gas heating and increasing the costs of $N \equiv N$ bond dissociation, a number of methods were proposed in the literature to reach high vibrational excitation of N_2 in plasmas operating at high pressure [30, 42, 49, 52].

In summary, depending on the mean electron energy or T_e, plasma-induced NF processes can be dominated by (i) elastic collisions, typical for thermal plasmas,

(ii) electron impact dissociation, (iii) vibrational excitation, and/or (iv) electronic excitation. The contribution of these processes is defined by the energy of the electrons, which can be tuned based on the type of electrical discharge, specifically the value of E/n required to sustain the discharge and heat the electrons. It is, therefore, convenient to classify electrical discharges based on the E/n value, as given in Table 7.3. As given in Tables 7.2 and 7.3 for an N_2 atmosphere, electronically excited species (e.g., $N_2(A^3\Sigma_u^+$, $B^3\Pi_g$, $a^1\Pi_g$, or $C^3\Pi_u)$ are typically produced when the E/n strength exceeds 100 Td. This mechanism of N_2 excitation is dominant in dielectric barrier discharges (DBDs), corona discharges (where photon-related processes also occur), and short-pulse plasmas. Meanwhile, favorable vibrational excitation, i.e., $N_2(X^1\Sigma_g^+, v)$ formation, occurs in plasmas with E/n < 100 Td, such as those in glow discharge mode (mostly direct current), radiofrequency (RF), and microwave (MW) plasmas, as described in Table 7.3. It is generally assumed that both electronic excitation and vibrational excitation can be initiated in pulsed plasmas (pulse duration from 10 μs to 100 ms). At E/n below 5 Td, elastic collisions become dominant, and plasmas tend to transition to thermal equilibrium.

7.3 The Effect of Water on Plasma Properties and N_2 Activation Processes

The presence of water in the system changes plasma properties and leads to the formation of gaseous $H_xN_yO_z$ and liquefied NO_x^- and NH_4^+ products relevant to NF. It is well known that introducing water into a plasma complicates the discharge sustaining, i.e., the transition from a Townsend mode to corona, glow, or arc. The reason is related to the electron loss processes in the plasma bulk [53]. The presence of water shifts the balance of charged particles, directly affecting the electron concentration via electron-ion recombination (7.8) and electron attachment processes (7.9). The former is more crucial as H_3O^+ is a cluster ion $(H^+(H_2O)_n)$ that can also change the electric field distribution [53, 54].

$$H_3O^+ + e \rightarrow \text{products } (e.g., H + H_2O) \tag{7.8}$$

$$H_2O + e \rightarrow H_2 + O^- or\ OH + H^- \tag{7.9}$$

The formation of gaseous and liquefied products can occur in the gas and liquid phases as well as in the thin layer called the plasma/liquid interface [55]. The concentrations of the final N-containing products, meaning a reactor energy efficiency, are strongly correlated with the total plasma–water interface surface area and interaction time when plasma is in contact with a liquid. Figure 7.4 represents typical plasma–liquid reactor geometries, which are classified based on the plasma–water phase distribution, namely

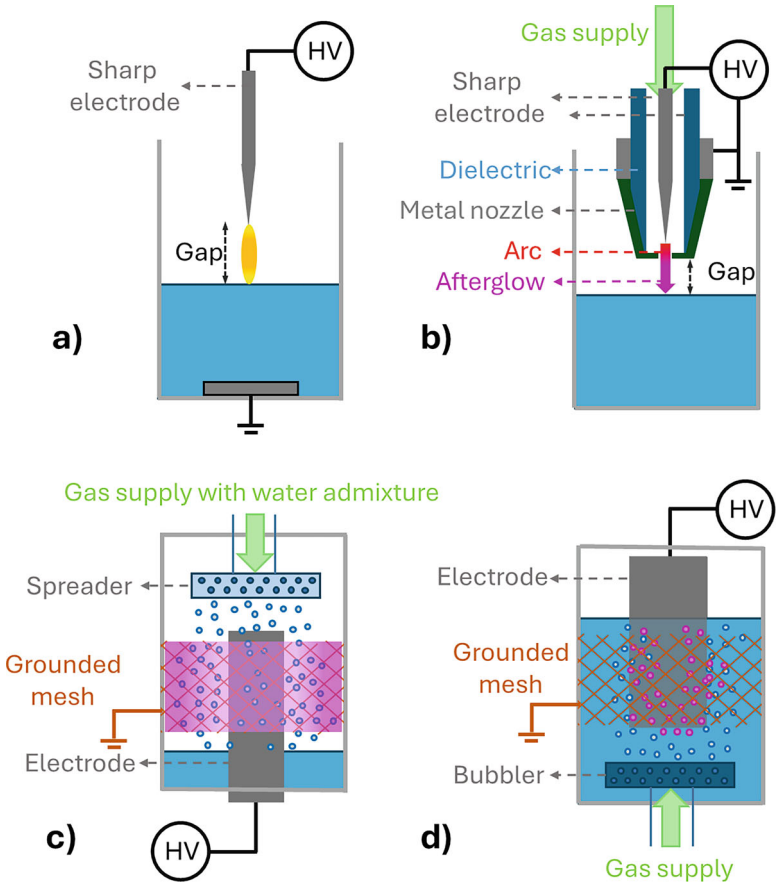

Fig. 7.4 Schematics of different plasma–liquid configurations and corresponding real setup images: (**a**) and (**b**) plasma-on-water; (**c**) water-in-plasma; (**d**) plasma-in-water

I. Plasma-on-water (Fig. 7.4a, b);
II. Water-in-plasma (Fig. 7.4c);
III. Plasma-in-water (Fig. 7.4d).

The plasma-above-water reactor, shown in Fig. 7.4a, b, has a low plasma–liquid contact area, mainly determined by the plasma column cross-section or plasma–liquid contact point area. In this case, a plasma can be ignited by using water as one of the electrodes (Fig. 7.4a) or sustained over water (Fig. 7.4b). Both configurations have different plasma physical properties that can significantly affect the NF process [56, 57]. From this point of view, using a liquid electrode sustains and diffuses plasma because ions transport a plasma current through the water electrode, having much smaller mobility than electrons in metals. This restricts the current through the system and prevents plasma thermalization (the glow-to-arc transition or streamer-

to-spark transition for pulsed plasmas) [58]. On the other hand, water has a drastically smaller secondary electron emission coefficient with respect to metals meaning a higher breakdown voltage. These two plasma configurations also show different chemical properties. The self-sustained discharges (Fig. 7.4b), for example, a plasma jet, generates reactive oxygen and nitrogen species (RONS) in the gas phase, and mostly long-lived species, e.g., NO_x, HNO_x, NH_3, H_2O_2, etc., are able to reach the surface of the water. Moreover, in this configuration, the water content in the gas phase remains low as only the plasma afterglow touches the water surface, which normally has a gas temperature close to room temperature. In contrast, a plasma with a liquid electrode (Fig. 7.4a) forms a plasma–liquid interaction surface [56, 57]. This determines a higher water concentration in the plasma bulk due to water evaporation and thermal and non-thermal spattering and involves short-lived species such as OH and OH_2 in forming NF products (more details will be given in the following section).

The interaction surface can be enlarged by spraying water into the plasma active zone or generating plasma in gas bubbles in the liquid, as shown in Fig. 7.4c, d [59]. Both of these systems have a large plasma–liquid interface, maximizing the effect of RONS on the NF process, and can be further upscaled by extending the plasma volume, creating a vortex gas or bubbles flow, and varying electrode configurations. The main disadvantages of these systems are the high breakdown voltage and energy losses due to Joule heating, which can be partly eliminated by adding porous layers to enhance the local electrical field and using dielectric barriers.

While publications on wet N_2 oxidation and N_2 reduction are relatively sparse compared to dry systems, interest in such processes has been increasing over the last 10 years. This rise is due to water being a green counterpart of CH_4 or H_2, providing H needed for both N_2 oxidation (HNO_3) and N_2 reduction (NH_3) processes [31, 60]. However, while the presence of the liquid phase is essential for the generation of nitrogen fixation products, its effect on process performance, particularly in terms of energy cost and product selectivity, remains unclear.

As introduced earlier, plasmas can provide four gas activation channels:

- Thermal activation
- Direct electron impact dissociation
- Activation via vibrational ladder climbing
- Electronic excitation

Here, the effect of water on each of these channels will be discussed from a physical standpoint. Although water can be introduced into the plasma zone through different approaches, they all represent the same plasma–liquid surface interaction, differing only in the interaction area. Therefore, the general effect of water on the excitation mechanisms is consistent across all water-containing systems, but the final contribution, of course, depends on the size of the plasma–liquid interaction area.

In the presence of high temperatures, part of the energy introduced into the system is also spent on water evaporation. Simple estimates indicate that evaporating 1 ml of water at 20 °C costs 0.05 MJ/mol, which is 25% of the energy cost of non-

equilibrium plasma NF estimations and 10% of the Haber-Bosch process. Therefore, the presence of water should indeed affect the thermal N_2 activation mechanisms, increasing its energy cost.

Comparing the electronic configurations of $N_2(X^1\Sigma_g^+, v)$ and $H_2O(X^1A_1, v_1, v_2, v_3)$ reveals that their vibrational levels have similar energy gaps (see Table 7.2 for details). This similarity triggers a vibrational–vibrational energy transfer process, quenching $N_2(X^1\Sigma_g^+, v > 0)$ through the reaction:

$$\begin{aligned} N_2\left(X^1\Sigma_g^+, v\right) + H_2O\left(X^1A_1, 0, 0, 0\right) \rightarrow N_2\left(X^1\Sigma_g^+, v-1\right) \\ + H_2O\left(X^1A_1, 0, 1, 0 \text{ or } 1, 0, 0\right) \end{aligned} \tag{7.10}$$

This means that water presence decreases N_2 vibrational excitation and negatively affects NF.

A similar situation is observed with the electronic excitation mechanism. Electronically excited levels of N_2 and H_2O are also close to each other (see Table 7.2). This proximity can cause electronic excitation of H_2O instead of N_2, decreasing N_2 activation through this mechanism. Moreover, the vibrational energy loading process in the ground electronic state is highly related to the higher electronic states through collisional/quenching processes, as presented via 7.11. This indicates that a decrease in the electronically excited state population can additionally reduce $N_2(X^1\Sigma_g^+, v > 0)$ vibrational excitation [61].

$$\begin{aligned} N_2\left(A^3\Sigma_g^+, B^3\Pi_g, C^3\Pi_u, v\right) + N_2\left(X^1\Sigma_g^+, v = 0\right) \rightarrow \\ \rightarrow N_2\left(A^3\Sigma_g^+, B^3\Pi_g, C^3\Pi_u, v-x\right) + N_2\left(X^1\Sigma_g^+, v+y\right) \end{aligned} \tag{7.11}$$

To summarize, the presence of water can thus adversely affect the NF process from a physical standpoint. Firstly, the plasma–liquid interface involves the transfer of H_2O from the liquid to the gas phase (evaporation), where electrons can react with it, further increasing the energy demands of the process. Secondly, the presence of water vapor can diminish vibrational excitation, hindering the activation of $N_2(X^1\Sigma_g^+, v > 0)$ molecules [53, 57]. Finally, the electronic activation of water can divert electron energy away from NF, specifically N_2(E) activation. Consequently, NF in the presence of a plasma–liquid interface can lead to a significant reduction in process energy efficiency (by some estimates, up to 20% [62]). On the other hand, some products of water dissociation, specifically OH radicals, can play a leading role in N_2 conversion chemistry, providing additional pathways for NF. Therefore, in the following section, the role of water in NF, focusing on the mechanisms of reactions initiated by plasma, will be discussed.

7.4 Plasma-Based Nitrogen Fixation Reaction Pathways and the Role of Water in It

An NF process in an electrical discharge has been conducted utilizing different N- and H-containing feedstocks introduced as gases [N_2, N_2 + O_2 (air), H_2, H_2O, CH_4, alcohols] and liquids (H_2O, alcohols). The presence of different phases does not bring consensus on the reaction locus for both HNO_3 and NH_3 formation. Opinions are divided between the liquid phase, gas phase, catalyst surface (if any is present), or the gas/liquid interface, based on the focus of the research. Following the objectives of this work, in this section, only the role of water in one-step plasma-based N_2 oxidation and N_2 reduction pathways will be discussed.

7.4.1 The Effect of Water on N_2 Oxidation in N_2:O_2 and N_2:O_2 + H_2O Feedstock Mixtures

NO_x formation requires a source of N and O. Air is the most obvious choice of feedstock owing to its abundance and accessibility. In dry N_2:O_2 gas mixtures, NO_x formation can be described as follows: feedstock activation (N_2, O_2)—initial product formation (NO)—further oxidation (NO_2), as presented in Table 7.4.

The plasma type strongly affects the occurring chemistry, namely during feedstock activation (7.12–7.16 for N_2, and 7.17–7.21 for O_2) and initial product formation stages (7.31–7.32). As discussed in Sect. 7.2.2, plasmas with a high electric field, i.e., E/n > 100 Td (such as DBDs), generate electronically excited species, while plasmas with E/n < 100 Td can initiate strong vibrational excitation (see Table 7.3 for details). In general, the generation of NO, a primary precursor for the formation of further, higher oxides, occurs via the so-called non-thermal Zeldovich mechanism. This term is often met in the plasma community, and it refers to reactions 7.31–7.32 driven by highly reactive species formed in plasma.

It is also generally accepted that the most energy-efficient pathway for NF is promoted by vibrational excitation of the ground state to N_2(X, v) (see Sect. 7.2.2). Vibrational excitation decreases the activation energy barrier for nitrogen dissociation, facilitating reaction 7.12 through 7.14, as given in Table 7.4. More importantly, for N_2 oxidation, the Zeldovich mechanism can be efficiently exploited by overpopulating the N_2 vibrational levels, and reaction 7.31 can be driven by N_2(X,v > 12). However, undesirable VT energy transfer processes often suppress vibrational excitation, which leads to a rise in gas temperature, inherently initiating NO formation following the thermal Zeldovich mechanism. This can be considered a waste of energy because thermal mechanisms are less efficient than their non-thermal counterparts. In addition, reverse processes (7.31–7.32) become more pronounced at high temperatures, restricting NO formation. This means that in warm plasmas [with E/n < 100 Td, such as gliding arcs (GA)], NO generation can occur through a combination of both non-thermal and thermal Zeldovich mecha-

Table 7.4 N_2 oxidation pathways in dry N_2:O_2 and N_2:O_2 + H_2O feedstocks. More information about the cross-sections and reaction rate constants can be found elsewhere [63, 80]

In dry N_2:O_2	In N_2:O_2 + H_2O	
Feedstock activation		
N_2 activation (common for both feedstocks)		
$e + N_2 \rightarrow N^{(*)} + N^{(*)} + e$		7.12
$e + N_2 \rightarrow N_2^*(v > 0) + e$		7.13
$e + N_2\left(X^1\Sigma_g^+, v\right) \rightarrow N + N^{(*)} + e$		7.14
$N_2^*(v) + N_2^*(v) \rightarrow N_2^*(v + n) + N_2^*(v - n)$		7.15
$e + N_2 \rightarrow N_2^*(E) + e$		7.16
O_2 activation (common for both feedstocks)		
$e + O_2 \rightarrow O + O^* + e$		7.17
$e + O_2 \rightarrow O + O^* + e$		7.18
$e + O_2 \rightarrow O_2^* + e$		7.19
$N_2^* + O_2 \rightarrow O + O^{(*)} + N_2^{(*)}$		7.20
$O_2 + O + M \rightarrow O_3 + M$		7.21
	H_2O activation In the gas phase	
	$e + H_2O \rightarrow OH + H + e$	7.22
	$O^* + H_2O \rightarrow OH + OH$	7.23
	$N_2^* + H_2O \rightarrow N_2 + H + OH$	7.24
	$H_2O \xrightarrow{UV\ irradiation\ 120-170\ nm} OH + H$	7.25
	$e + OH \rightarrow H + O + e$	7.26
	In the plasma–liquid interface	
	$OH + OH \rightarrow H_2O_2$	7.27
	$H_2O_2 + O \rightarrow HO_2 + OH$	7.28
	$OH + O_3 \rightarrow HO_2 + O_2$	7.29
	$OH + H_2O_2 \rightarrow HO_2 + H_2O$	7.30
Initial product formation (NO)		
(common for both feedstocks) $N_2^* + O \rightarrow NO + N$		7.31
(common for both feedstocks) $N^{(*)} + O_2^* \rightarrow NO + O$		7.32
	In the gas phase	
	$N^* + OH \rightarrow NO + H$	7.33
	In the plasma–liquid interface	
	$N + HO_2 \rightarrow NO + OH$	7.34
Further oxidation		
(common for both feedstocks) $NO + O + M \rightarrow NO_2 + M$		7.35
(common for both feedstocks) $NO + O_3 \rightarrow NO_2 + O_2$		7.36
	In the gas phase	
	$NO + H + M \rightarrow HNO + M$	7.37
	$NO_2 + HNO + M \rightarrow HNO_2 + NO$	7.38
	$NO + OH + M \rightarrow HNO_2 + M$	7.39
	$H_2O + NO_2 \rightarrow OH + HNO_2$	7.40
	$H_2O + NO_2 + NO \rightarrow HNO_2 + HNO_2$	7.41
	In the plasma–liquid interface	
	$NO_2 + O + M \rightarrow NO_3 + M$	7.42
	$HO_2 + NO_2 \rightarrow HNO_2 + O_2$	7.43
	$OH + NO_2 + M \rightarrow HNO_3 + M$	7.44
	$OH + NO_2 + M \rightarrow HNO_3 + M$	7.45
	$H_2O_2 + NO_2 + NO_2 \rightarrow HNO_3 + HNO_3$	7.46
	$HO_2 + NO + M \rightarrow HNO_3 + M$	7.47

nisms. However, the specific contribution of each mechanism remains uncertain and is subject to ongoing scientific debate.

The ultimate oxidation of NO to NO_2 in dry N_2:O_2 feedstock is shown in reactions 7.35 and 7.36. Ozone (O_3) production primarily occurs through the reaction $O_2 + O + M \rightarrow O_3 + M$, which consumes reactive oxygen atoms (M stands for the third body). O_3 is crucial for the formation of NO_2; nevertheless, in plasmas with elevated gas temperatures, the significance of 7.36 diminishes as O_3 becomes unstable at high temperatures. It is worth noting that reaction $N + O_3 \rightarrow NO + O_2$ cannot contribute at the initial oxidation state stage due to its low reaction rate constant [63].

The effect of the N_2:O_2 ratio on the production rate (PR) and energy cost (EC) was investigated in various plasma systems, including MW, DBD, nanosecond pulse, and GA [32, 43, 64, 65]. The best performance is consistently achieved with a gas mixture ratio of 1:1 (rather than 4:1 as in air). However, the enhancement in the yield of oxidation products is not significant, considering the energy expenses associated with the production of either pure N_2 or O_2.

The most industrial-relevant question is achieving the theoretical minimum EC of NF. It can be realized by utilizing the non-thermal Zeldovich mechanism, which is a key objective in the plasma community. Alongside direct NO_x formation, two common challenges are:

- minimizing its decomposition via reverse reactions;
- maximizing the fraction of gas treated by the plasma [64, 66–68].

These issues are often addressed by using pulsed spark plasmas [27, 28], incorporating specialized output gas nozzles (utilizing the adiabatic and Joule-Thomson effects to cool the gas through expansion) [69–71], modifying the gas flow dynamics [69, 71], and introducing an increased pressure to favor NO oxidation into NO_2 rather than NO_x decomposition [64].

For NF in the presence of water, the latter serves as a source of either O or O/H needed for NO_x or HNO_x formation, respectively (in this case, the reduction process can also take place, and it will be discussed in the following subsection). It must be noted that from an application point of view, the $N_2 + H_2O$ gas mixture is not very practical for N_2 oxidation because pure N_2 is a feedstock with added costs, and it requires pressure swing adsorption for separation from the air, and the absence of O_2 obviously reduces the contribution of the N_2 oxidation pathway in NF. Studies of $N_2 + H_2O$ systems mostly aim for the fundamental purpose of defining the role of water in NF by reducing the number of reactants, i.e., simplifying the chemistry.

When liquid H_2O is introduced into the system, NF products accumulate in the liquid phase. These products may include NH_3 in the form of NH_4^+, as well as oxidation products of nitrogen, such as nitrite (NO_2^-) and nitrate (NO_3^-) ions. Therefore, the plasma-based synthesis of reactive oxygen species (ROS) and reactive nitrogen species (RNS) in water is often referred to as plasma-treated water (PTW) or plasma-activated water (PAW) [72].

There is no general agreement on the reaction locus for NO_x formation in the presence of H_2O. Opinions are divided among the gas phase, plasma–liquid

interface, and liquid phase. It has already been introduced in Sect. 7.3 that an increase in NF species production rate can be achieved by increasing the plasma–liquid surface area [20]. Considering this, designs with an increasing interface surface have been intensively studied: aerosol droplets [23], water film, and vapor [24], and plasmas with a larger plasma–liquid interaction surface [20]. The source of the reactive species responsible for plasma–liquid chemistry is still under debate. Overall, conclusions about the reaction locus strongly depend on the reactor arrangement and the method of water introduction. Given that NF chemistry in the presence of H_2O is still under debate, NF chemistry in three distinguishable cases: (i) water in the gas phase, (ii) plasma–liquid interface, and (iii) in the bulk will be discussed hereafter.

For all cases, the feedstock activation stage is the same, and H_2O homolytically dissociates into H and OH (7.22) under the action of electron impact and reaction with electronically excited states of O^* and N_2^* (7.23 and 7.24, respectively) [73, 74]. Photodissociation of H_2O (7.25) may also take place in plasmas, especially with high E/n values observed for a corona discharge or a DBD [75]. Furthermore, the full dissociation of H_2O into H and O may also be considered following reaction 7.26. However, the probability of this latter process should be small for two main reasons. Firstly, it involves a two-step process: two electron impact reactions (7.22 and 7.26) or heavy-particle (7.23 or 7.24) and electron impact (7.26). Secondly, the reaction rate will be determined by the concentration of reactants, especially OH and electrons, which may be in limited supply. The concentration of the latter strongly depends on the plasma type (n_e(DBD) < 10^{21} m^{-3}, and n_e(spark) < 10^{24} m^{-3}, at atmospheric pressure conditions).

In the gas phase of an N_2:O_2 + H_2O system, NO formation should dominantly follow the reactions 7.31–7.32 and 7.33. However, in the N_2 + H_2O gas medium, the precursor formation process 7.32 is significantly suppressed due to the lack of O_2 in the gas mixture but can be replaced through 7.33, involving OH radicals. The effect of the latter on NO formation in the gas phase has been shown through experiments in many studies [23, 32, 62, 65, 73, 74, 76].

In addition to 7.35–7.36, further oxidation processes in the gas phase can be enhanced by the reactions 7.37–7.41. In the N_2 + H_2O gas mixture, due to a shortage of O/O_2, the selectivity of stable products is strongly shifted toward HNO_2 formation because further NO oxidation is mostly governed by OH radicals (7.39) [77]. Several important points should be noted here. Due to its high reactivity, among different products of the NF process, HNO cannot be isolated as a product. It reacts rapidly with other molecules or undergoes decomposition into simpler compounds. Therefore, HNO is primarily encountered as an intermediate in chemical reactions. Nitric acid (HNO_3) formation in the gas phase can occur only under very specific conditions, such as low pressure and temperature. At atmospheric pressure in the gas phase, HNO_3 can be formed as $OH + NO_2 + M \rightarrow HNO_3 + M$ with $k(298\ K) = 4.7 \cdot 10^{-11}$ cm^3 s^{-1} (reduced to the second-order reaction) [63], which decreases with temperature, slowing it down. Meanwhile, one of the major HNO_3 removal processes, namely $OH + HNO_3 \rightarrow H_2O + NO_2$, has $k(298\ K) = 2 \cdot 10^{-13}$ cm^3 s^{-1} and exponentially

increases with temperature. Therefore, HNO_3 is unstable and prone to decompose, ending up as NO_2. The same effect can take place with NO_3, whose removal processes, namely $NO_3 + O \rightarrow O_2 + NO_2$ and $NO + NO_3 \rightarrow NO_2 + NO_2$, are faster than the formation. The NF chemistry at the plasma–liquid interface remains unclear and has yet to be completely revealed. The lack of systematic studies is the primary reason for this uncertainty. Most research focuses on the behavior of a few radicals, neglecting the full range of possibilities. Furthermore, studies of chemical pathways are frequently limited by the absence of comprehensive computational chemical modeling. The unavailability of essential reaction rate constants (or their significant uncertainty), coupled with the challenges of aligning the three phases where water exists in different states (gas phase—vapor, plasma–liquid interface—mist, liquid phase—water bulk), pose significant barriers to developing a chemical kinetics model for plasma–liquid systems. While some works address the chemistry in such systems, focusing on gas chemistry, plasma–liquid interface chemistry, and liquid chemistry separately, much more research is needed for further advancements [78, 79].

Due to the high concentration of gaseous H_2O at the plasma–liquid interface region, its activation following reactions 7.22–7.26 becomes more significant than in the gas phase, increasing the OH concentration. Moreover, this activation can significantly enhance the production of reactive species such as hydroxyl peroxide (H_2O_2) and hydroperoxyl radical (HO_2) via reactions 7.27–7.30. The latter opens an additional pathway for precursor formation, namely NO (7.34). Finally, the abundance of OH, H_2O_2, and HO_2 can further boost HNO_2 formation (7.43) and, more importantly, facilitate the formation of HNO_3 through reactions 7.44–7.47 at the plasma–liquid interface. Besides these often-addressed reactions, the possibility of other reactions, such as $NO + OH^-$, is unknown, requiring further investigation [75].

The plasma–liquid interface primarily serves as the site for solvation reactions, following Henry's law. The solubility of $(H)NO_x$ components, arranged from weakest to strongest, follows $NO \rightarrow NO_2 \rightarrow NO_3 \rightarrow HNO_2 \rightarrow HNO_3$. Considering the high Henry's constants of HNO_3 and NO_3, the plasma–liquid interface can indeed be regarded as the crucial site for their formation (7.42, 7.44–7.47), where they are initially generated and then solvated.

The products of N_2 oxidation in liquids are NO_2^- and NO_3^- ions. Liquid-phase chemistry in this context has been extensively researched, with numerous reviews available on this topic [58, 75, 81, 82]. However, uncertainty persists regarding the reaction pathways that lead to the formation of these products. The liquid phase becomes increasingly dominated by NO_2^- in plasmas with high concentrations of HNO_2 and NO in the gas phase, achievable in $N_2 + H_2O$ and dry N_2:O_2 feedstocks, respectively. Meanwhile, the selectivity shift toward NO_3^- is pronounced in plasmas with large plasma–liquid interface areas due to the elevated solubility of HNO_3 and NO_3 and at increased concentrations of NO_2. The latter, high NO_2 concentrations, are most pronounced in dry N_2:O_2 plasmas, reaching 50–70% selectivity, and can be further enhanced up to 100% by introducing an

additional oxidation source, such as ozone, or performing the synthesis at elevated pressure [64, 83].

Focusing on plasma-based NF for fertilizer production, it is imperative to maintain a low concentration of NO_2^- in the output solution due to its detrimental effects on plants. Elevated NO_2^- levels can disrupt various cellular processes and inhibit essential enzymes, leading to oxidative stress, chlorosis (yellowing of leaves), and even plant death. From a chemical perspective, the most efficient method to convert NO_2^- present in the output into NO_3^- is through a reaction involving H_2O_2. The latter can be effectively generated in plasmas with water presence at high electronic excitation degrees and low gas temperatures, e.g., in plasmas at E/n > 100 Td. However, in plasmas with vibrational excitation, such as a GA (E/n < 100 Td), the high temperature inhibits H_2O_2 generation. In such cases, NO_2^- can be converted into NO_3^- by bubbling O_2 gas through the liquid.

To summarize, the presence of water in the plasma zone, specifically at the plasma–liquid interface, enables more diverse chemistry and ensures more chemical pathways for initial product formation and further oxidation. Table 7.5 presents the typical products of plasma-based N_2 oxidation in various atmospheres and their respective performances. The main role of water in the system is to shift selectivity toward HNO_x generation. Similar to the Ostwald process, the ultimate aim of plasma-based N_2 oxidation for fertilizer production is to generate HNO_3. This is achievable only if HNO_3 is preserved in water as NO_3^-, making the selectivity of its generation crucial and a primary focus in the field. Considering this, most studies in the literature focus on tuning N_2 oxidation selectivity. Examining the latter from an energy cost perspective requires considering several important plasma parameters,

Table 7.5 Typical plasma-based NF performance in dry N_2:O_2, N_2:O_2 + H_2O, and N_2 + H_2O feedstocks, considering an excess of the reactants

	Selectivity [83, 84]	
Feedstock	In gas phase	In liquid phase
Dry N_2:O_2 (air)	NO, NO_2	NO_2^-/NO_3^- > 1
N_2:O_2 (air) + H_2O	HNO_2, NO, NO_2	NO_2^-/NO_3^- < 1, NH_4^+(low)
N_2 + H_2O	HNO_2, NH_3	NO_2^-/NO_3^- < 1, NH_4^+
Performance		
Plasma type	EC, MJ/mol	PR, g/h
N_2 oxidation in N_2:O_2 feedstock		
E/n < 100 Td (Arc, GA, MW, pulsed plasmas) [64]	1–10	<100
E/n > 100 td (DBD, (pulsed) corona discharge) [16]	10–100 s	≈1
N_2 reduction		
E/n > 100 Td (DBD in N_2 + H_2O)	10–1000 s	≈1 mg/h
E/n > 100 Td (DBD + catalyst in N_2:O_2 + H_2O) [16]	1–10	1–10 s mg/h

namely plasma power, plasma temperatures, and the detection of products in both gas and liquid phases. The number of available studies providing a quantitative comparison of plasma systems with and without water is limited. However, some studies indicate that the N_2 oxidation process in a spark plasma on water is almost 16% [62] less efficient than in dry air. This result was attributed to energy loss due to water evaporation, a decrease in N_2 activation (quenching of N_2^* by water molecules), and energy losses due to water activation.

7.4.2 The Effect of Water on N_2 Reduction in $N_2 + H_2O$ and N_2:$O_2 + H_2O$ Feedstock Mixtures

Another interesting concept receiving a lot of attention is the use of H_2O either as a gas, liquid, or vapor as an abundant, green H source for the reduction process [55, 82]. In this case, thermal plasmas have found more use, e.g., in treating a liquid surface [82]. The N_2 and H_2O activation can occur in the thermal region of the plasma, while the initial product formation (NH, 7.48–7.52) and hydrogenation ($NH \rightarrow NH_3$, 7.53–7.56) may occur in the low-temperature afterglow. The N_2 activation will follow the same reactions as in N_2 oxidation, 7.12–7.16 but predominantly through the interaction with the vibrationally excited $N_2(X,v)$. It must be noted that in the absence of O_2, H_2O also simultaneously plays a role of O and H source. Therefore, in $N_2 + H_2O$ systems, two sets of processes can occur: N_2 reduction, as discussed here and presented in Table 7.6, and N_2 oxidation, as discussed in the previous subsection (Table 7.4).

Again, for the systems with H_2O, the reaction locus is a subject of debate and likely depends on a specific plasma–liquid configuration. Still, in the case of systems

Table 7.6 N_2 reduction pathways in $N_2 + H_2O$ feedstock. More information about the cross-sections and reaction rate constants can be found elsewhere [63, 80]

In $N_2 + H_2O$	
Feedstock activation	
N_2 activation: 7.12–7.16 (see Table 7.4)	
H_2O activation: 7.22–7.30 (see Table 7.4)	
Initial product formation (NH)	
$N + H \rightarrow NH$	*7.48*
$N_2^* + H \rightarrow NH + N$	*7.49*
$N^* + H_2 \rightarrow NH + H$	*7.50*
$N + OH \rightarrow NH + O$	*7.51*
$N_2^* + H_2O \rightarrow NH + N + OH$	*7.52*
Further hydrogenation	
$NH + H \rightarrow NH_2$	*7.53*
$NH + OH \rightarrow NH_2 + O$	*7.54*
$NH_2 + H \rightarrow NH_3$	*7.55*
$NH + H_2 \rightarrow NH_3$	*7.56*

comprised of plasma interacting with a liquid interface, extracting H from the liquid surface is considered the rate-limiting step for NH_3 formation in plasma–liquid systems [20]. To overcome this limitation, an additional activation mechanism via UV radiation of the water surface is a method used to increase the available H^+ at the plasma–liquid surface through 7.25, resulting in a more efficient hydrogenation. It can increase NH_4^+ formation (up to four-fold) compared to conditions without UV [20, 26, 85].

Unfortunately, although $N_2 + H_2O$ plasma systems are characterized by a rich environment with a variety of reactive species, namely additional OH and H_2O_2, these species also have negative effects on NH_3 or NH_4^+ generation from a physical and chemical point of view. First of all, the presence of water in the plasma zone initiates the quenching of vibrationally excited N_2(X,v) and electronically excited N_2(E) [53, 57, 74]. This decreases the N_2 activation efficiency. Secondly, at non-thermal conditions, OH is "wasted" on H_2O_2 generation (7.27) instead of contributing to NH_3 production, while at thermal conditions, OH radicals can trigger back reactions $OH + NH \rightarrow H + HNO$ and $OH + NH_2 \rightarrow H_2O + NH$, which negatively affect NH and NH_2 generation [73]. Furthermore, even assuming the complete two-step dissociation of H_2O into H + H + O (7.22–7.24, 7.26) from which both H react to form NH_x, the required O-H bond dissociation energy in H_2O is 4.81 eV (464 kJ/mol), whereas in H_2 it is 4.52 eV (436 kJ/mol). This means that to produce the same amount of NH_3, more energy is inherently required when using H_2O instead of H_2. This is clearly seen when looking at the performance of $N_2 + H_2O$ plasma systems with respect to their $N_2 + H_2$ counterparts, where the EC is two orders of magnitude higher, and the PR is two orders of magnitude lower for $N_2 + H_2O$ systems.

Interestingly, $N_2 + H_2O$ reduction with H_2O vapor in the presence of a catalyst in a DBD plasma can reduce the contribution of the oxidation pathway and increase the contribution of the reduction pathway [86]. However, the practical importance of these systems for N_2 reduction is low due to their high EC and low PR [17].

From an application standpoint, the most desirable scenario for NF involves utilizing air as a source of nitrogen since it is readily available in abundance. However, transitioning from pure N_2 to an air plasma leads to a dramatic decrease in NH_3 production [20]. Moreover, the selectivity of NF shifts toward N_2 oxidation, as detailed in Sect. 7.4.1 and given in Table 7.4. In fact, in nearly all works found in literature, the only products of the $N_2 + O_2$ (air) + H_2O reactive plasma systems are NO_x and HNO_x [82]. Nonetheless, NH_3 formation may occur even in $N_2 + O_2$ (air) + H_2O systems, with and without a catalyst. These works reveal an important point to consider: if the plasma feed gas contains large amounts of H_2O vapor, the formed NH_3 will react with the formed HNO_2, yielding NH_4NO_2, which is unstable at ambient conditions and decomposes back to N_2 and H_2O [77]. Thus, a high humidity content can be detrimental to plasma NF via oxidation into NO_x. These are two examples that focus either on DBD plasma catalysis with H_2O vapor or pulsed spark plasma with a very low duty cycle (i.e., inherently low throughput) [77, 87], motivating more research on this topic.

7.5 Outlook and Perspectives

Plasma-based NF technology is an attractive prospect for small-scale fertilizer production that can provide access to fixed atmospheric N_2, synthesizing either (H)NO_x or NH_3, enabling on-site fertilizer production, such as ammonium nitrate. This chapter discusses the role of water in this process, highlighting that water is an eco-friendly replacement for CH_4 or H_2 currently used in the industry to supply hydrogen for synthesis. The analysis provided here allows us to confidently conclude that the presence of water in the plasma zone introduces more disadvantages than process improvements.

The higher energy cost of NF in the presence of water is attributed to energy losses from water evaporation, quenching of vibrationally and electronically excited N_2 molecules by water, which are the main driving force of the NF process, and changes in NF kinetics. The latter indicates that the extended chemistry set in the presence of water cannot overcome the plasma's physical restrictions discussed in Sects. 7.2 and 7.3, and the extended Zeldovich mechanism involving OH radicals and its products in the presence of water might be less efficient than the Zeldovich mechanism under non-equilibrium plasma conditions (see Sect. 7.4).

Considering this, N_2 oxidation should be conducted in a dry air atmosphere due to its abundance. The process results in the formation of NO_x, which can be further bubbled in water, resulting in NO_x^-. However, it is imperative to maintain high NO_2 selectivity in the gas phase to ensure an NO_3^- dominant solution. For this reason, selectivity can be tuned by changing plasma parameters (e.g., pressure) or introducing an extra oxidation source, such as O_3.

Regarding N_2 reduction, it can be concluded that a one-step plasma process involving only $N_2 + H_2O$ or N_2:$O_2 + H_2O$ is unlikely to be developed for commercial needs in the coming decades. Among the most basic reasons are the energy demands of the N_2 separation unit to create a pure N_2 atmosphere and the decisive shift toward N_2 oxidation in an N_2:$O_2 + H_2O$ feedstock.

A direct one-step plasma N_2 reduction approach demonstrates poor performance in terms of both PR and EC, rendering it impractical (see Table 7.5). Still, several plasma-involving methods can overcome the low efficiency of N_2 reduction. One promising approach is electrochemical conversion, which uses plasma-synthesized NO_x to convert it into NH_4^+ later [88, 89]. This technology shows the most promising results in terms of energy consumption and yield of NH_4^+ (see Table 7.5). More importantly, this method can be straightforwardly applied to NH_4NO_3 synthesis. It involves adding a couple of electrodes in water, collecting liquefied NO_x^- species, and partially converting them into NH_4^+, resulting in a water solution containing both NO_3^- and NH_4^+, i.e., a ready-to-use fertilizer.

Another option is to recycle NH_3 stored in cattle and pig manure. Manure is rich in nitrogen (2–8.1 g/kg) [90] with about 70% of it in the form of NH_4^+, although this content decreases over time. The volatilization of ammonia from manure is estimated to be tens of kilograms per hectare of fertilized soil [91]. The NH_3-enriched air from cattle or pig housing or manure storage areas can be bubbled

through a water repository, dissolving in water as NH_4^+. A similar laboratory study has already been demonstrated [92]. This approach is superior to others presented here because it does not require electrical power for synthesis, and the NH_3 content in the carrier gas is significantly higher than what can be achieved through artificial methods.

Nevertheless, the plasma–liquid interface system arrangement is worth investigating because many questions remain unanswered, particularly concerning NF. The NF chemistry at the plasma–liquid interface remains largely unexplored due to a lack of systematic studies. Most research focuses on a few radicals, ignoring the full spectrum of possibilities. Additionally, thorough computational chemical modeling is often missing, with significant gaps in reaction rate constants and difficulties in matching water's different states, including gas, plasma–liquid, and bulk. These challenges hinder the development of a comprehensive chemical kinetics model for plasma–liquid systems. While some studies address gas chemistry, plasma-liquid interface chemistry, and liquid chemistry separately, more research is needed to advance this field.

Future studies should critically examine N_2 reduction pathways through experimental investigation and plasma modeling in an N_2:O_2 + H_2O feedstock. Combining these approaches can help understand how to shift the NF process toward N_2 reduction under desirable conditions (air + water).

Finally, the effect of water on the vibrational excitation of N_2 is evident but unquantified. Investigating the balance between species has provided only comparative data, based on comparing two plasma systems. More research could help define, for example, the optimal amount of water admixture in the gas phase to promote NF pathways while minimizing N_2 quenching.

Acknowledgement This research was supported by the Excellence of Science (EOS) FWO-FNRS project NITROPLASM (EOS ID 30505023) and by the FWO through a grant for a short research stay outside Europe (FWO ID K207621N).

References

1. T. Wrońska-Nofer, J. Palus, W. Krajewski, J. Jajte, M. Kucharska, J. Stetkiewicz, W. Wasowicz, K. Rydzyński, Mutat. Res.– Fund. Mol. Mech. Mutag. **666**, 39 (2009)
2. P.M. Vitousek, J.D. Aber, R.W. Howarth, G.E. Likens, P.A. Matson, D.W. Schindler, W.H. Schlesinger, D.G. Tilman, Ecol. Appl. **7**, 737 (1997)
3. A. Ito, K. Nishina, K. Ishijima, S. Hashimoto, M. Inatomi, Prog Earth Planet Sci **5**, 13 (2018)
4. C. Martínez-Espinosa, S. Sauvage, A. Al Bitar, P.A. Green, C.J. Vörösmarty, J.M. Sánchez-Pérez, Sci. Total Environ. **754**, 142398 (2021)
5. N. Lehnert, in *Feeding the World in the 21st Century: Grand Challenges in the Nitrogen Cycle* (2015), pp. 3–37
6. J.N. Galloway, E.B. Cowling, Ambio **31**, 64 (2002)
7. J.W. Erisman, M.A. Sutton, J. Galloway, Z. Klimont, W. Winiwarter, Nat. Geosci. **1**, 636 (2008)

8. E. A. A. Umweltbundesamt, *Production of Ammonia, Nitric Acid, Urea and N-Fertilizer* (2017)
9. C. P. Chanway, R. Anand, and H. Yang, in *In Advances in Biology and Ecology of Nitrogen Fixation* (InTechOpen, 2014)
10. B.S. Patil, Q. Wang, V. Hessel, J. Lang, Catal. Today **256**, 49 (2015)
11. C. Smith, A.K. Hill, L. Torrente-Murciano, Energy Environ. Sci. **13**, 331 (2020)
12. N. Cherkasov, A.O. Ibhadon, P. Fitzpatrick, Chem. Eng. Process. Process Intensif. **90**, 24 (2015)
13. J. Humphreys, R. Lan, S. Tao, Adv. Energy Sustain. Res. **2**, 2000043 (2021)
14. S. Huang, W. Lv, S. Bloszies, Q. Shi, X. Pan, Y. Zeng, Field Crop Res. **192**, 118 (2016)
15. K.H.R. Rouwenhorst, Y. Engelmann, K. Van't Veer, R.S. Postman, A. Bogaerts, L. Lefferts, Green Chem. **22**, 6258 (2020)
16. K.H.R. Rouwenhorst, F. Jardali, A. Bogaerts, L. Lefferts, Energy Environ. Sci **14**, 2520 (2021)
17. Y. Gorbanev, I. Fedirchyk, A. Bogaerts, Curr. Opin. Green Sustain. Chem. **47**, 100916 (2024)
18. V.D. Rusanov, A.A. Fridman, G.V. Sholin, Soviet Phys. – Uspekhi **24**, 447 (1981)
19. J. Hong, S. Prawer, A.B. Murphy, IEEE Trans. Plasma Sci. **42**, 2338 (2014)
20. T. Haruyama, T. Namise, N. Shimoshimizu, S. Uemura, Y. Takatsuji, M. Hino, R. Yamasaki, T. Kamachi, M. Kohno, Green Chem. **18**, 4536 (2016)
21. S. Kumar, N. Singh, R. Prasad, Renew. Sust. Energ. Rev. **14**, 1830 (2010)
22. E. Morais, A. Bogaerts, Plasma Process. Polym. **21**, e2300149 (2024)
23. J.R. Toth, N.H. Abuyazid, D.J. Lacks, J.N. Renner, R.M. Sankaran, ACS Sustain. Chem. Eng. **8**, 14845 (2020)
24. Y. Gorbanev, E. Vervloessem, A. Nikiforov, A. Bogaerts, ACS Sustain. Chem. Eng. **8**, 2996 (2020)
25. S. Yoshida, N. Murakami, Y. Takatsuji, T. Haruyama, Green Chem. **25**, 579 (2022)
26. T. Sakakura, S. Uemura, M. Hino, S. Kiyomatsu, Y. Takatsuji, R. Yamasaki, M. Morimoto, T. Haruyama, Green Chem. **20**, 627 (2018)
27. E. Vervloessem, Y. Gorbanev, A. Nikiforov, N. De Geyter, A. Bogaerts, Green Chem. **24**, 916 (2022)
28. N. Britun, V. Gamaleev, M. Hori, Plasma Sources Sci. Technol. **30**, 08LT02 (2021)
29. X. Pei, D. Gidon, Y.J. Yang, Z. Xiong, D.B. Graves, Chem. Eng. J. **362**, 217 (2019)
30. E. Vervloessem, M. Aghaei, F. Jardali, N. Hafezkhiabani, A. Bogaerts, ACS Sustain. Chem. Eng. **8**, 9711 (2020)
31. Z. Liu, Y. Tian, G. Niu, X. Wang, Y. Duan, ChemSusChem **14**, 1507 (2021)
32. N.C. Roy, C. Pattyn, A. Remy, N. Maira, F. Reniers, Plasma Process. Polym. **18**, e2000087 (2021)
33. B. Tarabová, P. Lukeš, M. Janda, K. Hensel, L. Šikurová, Z. Machala, Plasma Process. Polym. **15**, e1800030 (2018)
34. X. Tang, J. Wang, H. Yi, S. Zhao, F. Gao, C. Chu, Plasma Chem. Plasma Process. **38**, 485 (2018)
35. R.J. Wandell, H. Wang, R.K.M. Bulusu, R.O. Gallan, B.R. Locke, Plasma Chem. Plasma Process. **39**, 643 (2019)
36. C. Tendero, C. Tixier, P. Tristant, J. Desmaison, P. Leprince, Spectrochim. Acta Part B At. Spectrosc. **61**, 2 (2006)
37. V.N. Ochkin, *Spectroscopy of Low Temperature Plasma* (John Wiley & Sons, Weinheim, 2009)
38. G. Herzberg, *Molecular Spectra and Molecular Structure* (Litton Educational Publishing, New York, 1950)
39. C.N. Banwell, E.M. McCash, *Fundamentals of Molecular Spectroscopy* (Indian Edition, 2017)
40. A. Fridman, L.A. Kennedy, *Plasma Physics and Engineering* (CRC Press, 2004)
41. A. Bogaerts, E.C. Neyts, ACS Energy Lett. **3**, 1013 (2018)
42. T. Kim, S. Song, J. Kim, R. Iwasaki, Jpn. J. Appl. Phys. **49**, 126201 (2010)
43. O.S. Bahnamiri, C. Verheyen, R. Snyders, A. Bogaerts, N. Britun, Plasma Sources Sci. Technol. **30**, 065007 (2021)
44. M. Rubio, L. Serrano-Andŕs, M. Merchán, J. Chem. Phys. **128**, 104305 (2008)

45. K. Hänninen, Environ. Ecol. Res. **6**, 74 (2018)
46. M. Lopez del Puerto, M.L. Tiago, I. Vasiliev, J.R. Chelikowsky, Phys. Rev. A **72**, 052504 (2005)
47. D. Burnette, A. Montello, I.V. Adamovich, W.R. Lempert, Plasma Sources Sci. Technol. **23**, 45007 (2014)
48. M. Uddi, N. Jiang, I.V. Adamovich, W.R. Lempert, J. Phys. D. Appl. Phys. **42**, 075205 (2009)
49. C. Richards, E. Jans, I. Gulko, K. Orr, I.V. Adamovich, Plasma Sources Sci. Technol. **31**, 034001 (2022)
50. E.R. Jans, K. Frederickson, T.A. Miller, I.V. Adamovich, J. Mol. Spectrosc. **365**, 111205 (2019)
51. A. Montello, Z. Yin, D. Burnette, I.V. Adamovich, W.R. Lempert, J. Phys. D. Appl. Phys. **46**, 464002 (2013)
52. P. Barboun, P. Mehta, F.A. Herrera, D.B. Go, W.F. Schneider, J.C. Hicks, ACS Sustain. Chem. Eng. **7**, 8621 (2019)
53. M. Capitelli, C.M. Ferreira, B.F. Gordiets, A.I. Osipov, *Plasma Kinetics in Atmospheric Gases* (Springer Series on Atomic, Optical, and Plasma Physics, 2013)
54. J. Jiang, Y. Aranda Gonzalvo, P.J. Bruggeman, Plasma Chem. Plasma Process. **41**, 1569 (2021)
55. P.J. Bruggeman, M.J. Kushner, B.R. Locke, J.G.E. Gardeniers, W.G. Graham, D.B. Graves, R.C.H.M. Hofman-Caris, D. Maric, J.P. Reid, E. Ceriani, D. Fernandez Rivas, J.E. Foster, S.C. Garrick, Y. Gorbanev, S. Hamaguchi, F. Iza, H. Jablonowski, E. Klimova, J. Kolb, F. Krcma, P. Lukes, Z. MacHala, I. Marinov, D. Mariotti, S. Mededovic Thagard, D. Minakata, E.C. Neyts, J. Pawlat, Z.L. Petrovic, R. Pflieger, S. Reuter, D.C. Schram, S. Schröter, M. Shiraiwa, B. Tarabová, P.A. Tsai, J.R.R. Verlet, T. Von Woedtke, K.R. Wilson, K. Yasui, G. Zvereva, Plasma Sources Sci. Technol. **25**, 053002 (2016)
56. P. Heirman, W. Van Boxem, A. Bogaerts, Phys. Chem. Chem. Phys. **21**, 12881 (2019)
57. I. Sremački, M. Gromov, C. Leys, R. Morent, R. Snyders, A. Nikiforov, Plasma Process. Polym. **17**, e1900191 (2019)
58. P. Bruggeman, C. Leys, J. Phys. D. Appl. Phys. **42**, 053001 (2009)
59. J.G. Haase, L.H. Leung, P.D. Evans, Coatings **9**, 14 (2019)
60. J. Hong, T. Zhang, R. Zhou, L. Dou, S. Zhang, R. Zhou, B. Ashford, T. Shao, A.B. Murphy, K.K. Ostrikov, P.J. Cullen, Green Chem. **24**, 7458 (2022)
61. Y. Wu, C.M. Limbach, A.A. Tropina, R.B. Miles, AIAA Scitech 2019 Forum 2066 (2019)
62. M. Gromov, N. Kamarinopoulou, N. De Geyter, R. Morent, R. Snyders, D. Vlachos, P. Dimitrakellis, A. Nikiforov, Green Chem. **24**, 9677 (2022)
63. J.A. Manion, R.E. Huie, R.D. Levin, D.R. Burgess Jr., V.L. Orkin, W. Tsang, W.S. McGivern, J.W. Hudgens, V.D. Knyazev, D.B. Atkinson, E. Chai, A.M. Tereza, C.Y. Lin, T.C. Allison, W.G. Mallard, F. Westley, J.T. Herron, R.F. Hampson, H. Frizzell, NIST chemical kinetics database, NIST standard reference database. **17**, 20899 (2024)
64. I. Tsonev, C. O'Modhrain, A. Bogaerts, Y. Gorbanev, ACS Sustain. Chem. Eng. **11**, 1888 (2023)
65. J. Liu, L. Nie, D. Liu, X. Lu, Plasma Process. Polym. **21**, 2300153 (2024)
66. S. Eyde, Ind. Eng. Chem. **4**, 771 (1912)
67. F. Jardali, S. Van Alphen, J. Creel, H. Ahmadi Eshtehardi, M. Axelsson, R. Ingels, R. Snyders, A. Bogaerts, Green Chem. **23**, 1748 (2021)
68. W. Wang, B. Patil, S. Heijkers, V. Hessel, A. Bogaerts, ChemSusChem **10**, 2110 (2017)
69. S. Van Alphen, H.A. Eshtehardi, C. O'Modhrain, J. Bogaerts, H. Van Poyer, J. Creel, M.-P. Delplancke, R. Snyders, A. Bogaerts, Chem. Eng. J. **443**, 136529 (2022)
70. S. J. Andrews, H. Ogden, and J. Marshall, (1956)
71. I. Tsonev, H.A. Eshtehardi, M.-P. Delplancke, A. Bogaerts, Sustain Energy Fuels **8**, 2191 (2024)
72. F. Tampieri, Y. Gorbanev, E. Sardella, Plasma Process. Polym. **20**, e2300077 (2023)
73. A. Komuro, R. Ono, T. Oda, J. Phys. D. Appl. Phys. **46**, 175206 (2013)
74. M. Gromov, K. Leonova, N. Britun, N. De Geyter, R. Morent, R. Snyders, A. Nikiforov, React Chem Eng **7**, 1047 (2022)

75. S.Ž. Corina Bradu, K. Kutasi, M. Magureanu, N. Puac, J. Phys. D. Appl. Phys. **53**, 223001 (2020)
76. F. Fresnet, G. Baravian, L. Magne, S. Pasquiers, C. Postel, V. Puech, A. Rousseau, Plasma Sources Sci. Technol. **11**, 152 (2002)
77. E. Vervloessem, M. Gromov, N. De Geyter, A. Bogaerts, Y. Gorbanev, A. Nikiforov, ACS Sustain. Chem. Eng. **11**, 4289 (2023)
78. T. Murakami, in *APS Annual Gaseous Electronics Meeting Abstracts* (2023), pp. EW4-003
79. O. Sakai, S. Kawaguchi, T. Murakami, Jpn. J. Appl. Phys. **61**, 070101 (2022)
80. K.C. van't Veer, *Plasma Kinetics Modelling of Nitrogen Fixation: Ammonia Synthesis in Dielectric Barrier Discharges with Catalysts* (Universiteit Antwerpen & Université libre de Bruxelles, 2022)
81. A. Fridman, Y. Yang, Y.I. Cho, *Plasma Discharge in Liquid: Water Treatment and Applications* (CRC Press, 2012)
82. X. Zhao, Y. Tian, Cell Rep Phys Sci **4**, 101618 (2023)
83. D.K. Dinh, I. Muzammil, W.S. Kang, D. Kim, D.H. Lee, Plasma Sources Sci. Technol. **30**, 055020 (2021)
84. S. Li, J. Medrano Jimenez, V. Hessel, F. Gallucci, PRO **6**, 248 (2018)
85. Y. Kubota, K. Koga, M. Ohno, T. Hara, Plasma Fus. Res. **5**, 042 (2010)
86. H.M. Nguyen, F. Gorky, S. Guthrie, M.L. Carreon, Catal. Today **418**, 114141 (2023)
87. J. Feng, P. Ning, K. Li, X. Sun, C. Wang, L. Jia, M. Fan, ACS Sustain. Chem. Eng. **11**, 804 (2023)
88. C. Lee, Q. Yan, Curr Opin Electrochem **29**, 100808 (2021)
89. R.K. Sharma, H. Patel, U. Mushtaq, V. Kyriakou, G. Zafeiropoulos, F. Peeters, S. Welzel, M.N. Tsampas, ACS Energy Lett **6**, 313 (2021)
90. C. Font-Palma, C (Basel) **5**, 27 (2019)
91. M. Vilarrasa-Nogué, M.R. Teira-Esmatges, E. González-Llinàs, F. Domingo-Olivé, J.M. Villar, Sci. Total Environ. **724**, 137918 (2020)
92. Y. Zhu, Z. Xiong, M. Li, X. Chen, C. Lu, Z. Zou, Plasma Process. Polym. **18**, 1 (2021)